



GLOBAL JOURNAL OF RESEARCHES IN ENGINEERING: A
MECHANICAL AND MECHANICS ENGINEERING
Volume 18 Issue 2 Version 1.0 Year 2018
Type: Double Blind Peer Reviewed International Research Journal
Publisher: Global Journals
Online ISSN:2249-4596 Print ISSN:0975-5861

Effect of Local Dynamic Stability of a Ploydyne Cam with Translated Follower on Lyapunov Exponent Parameter over a Range of Speeds

By Dr. Louay S. Yousuf

Department of Mechanical Engineering San Diego State University

Abstract- This study quantized the relationship between local dynamic stability and the variation in cam rotational speeds. The dynamic analysis presents follower displacement driven by a cam rotating at a uniform angular velocity. There is a clearance between the follower and the guide. Maximum finitetime Lyapunov exponents were estimated to quantify local dynamic stability. Local stability of a follower attractor in the ydirection was shown to be achieved over multiple cam speeds. The variation in cam rotational speeds was associated with significant changes in Lyapunov exponent values. The numerical part of the dynamic model was investigated using Solid Works simulations. A Solid Works simulation is developed for the planar case using the block commands. Diferent follower guides' clearances have been used in the simulations. An experimental set up is developed to capture the general planar motion of the cam and follower. The measures the follower positions are obtained through high-resolution optical encoders (markers). A good agreement between numerical and experimental parts was obtained.

Keywords: *nonlinear dynamic, local stability, camfollower mechanism, lyapunov exponent.*

GJRE-A Classification: *FOR Code: 091399*



Strictly as per the compliance and regulations of:



© 2018. Dr. Louay S. Yousuf. This is a research/review paper, distributed under the terms of the Creative Commons Attribution-Noncommercial 3.0 Unported License <http://creativecommons.org/licenses/by-nc/3.0/>), permitting all non commercial use, distribution, and reproduction in any medium, provided the original work is properly cited.

Effect of Local Dynamic Stability of a Ploydyne Cam with Translated Follower on Lyapunov Exponent Parameter over a Range of Speeds

Dr. Louay S. Yousuf

Abstract- This study quantized the relationship between local dynamic stability and the variation in cam rotational speeds. The dynamic analysis presents follower displacement driven by a cam rotating at a uniform angular velocity. There is a clearance between the follower and the guide. Maximum finite-time Lyapunov exponents were estimated to quantify local dynamic stability. Local stability of a follower attractor in the y-direction was shown to be achieved over multiple cam speeds. The variation in cam rotational speeds was associated with significant changes in Lyapunov exponent values. The numerical part of the dynamic model was investigated using Solid Works simulations. A Solid Works simulation is developed for the planar case using the block commands. Diferent follower guides' clearances have been used in the simulations. An experimental set up is developed to capture the general planar motion of the cam and follower. The measures the follower positions are obtained through high-resolution optical encoders (markers). A good agreement between numerical and experimental parts was obtained.

Keywords: nonlinear dynamic, local stability, cam-follower mechanism, lyapunov exponent.

I. INTRODUCTION

A cam is a mechanical device which is used to transmit the motion to the follower. The proposed cam can be used in motor car camshafts to operate the engine valves. Recently, much research effort has been spent to study the contact-impact problem. UNLUSOY and TUMER, [1]. derived the exact quasi-linear solution to represent the non-linear behavior of cam mechanism at different cam speeds. The critical examination of the simulation has been made by using the equivalent viscous damper instead of Coulomb friction model. Hamidzadeh and Dehghani, [2]. used Hill's infinite determinant method to present a solution of linear, second-order, ordinary differential equation for different rotational speeds. They found that the system is stable for low values of cam rotational speeds. A few unstable regions are occurred when the speed is increased gradually. The effect of both operational speed and damping on the dynamic stability has been determined. Tounsi et-al, [3] presented the multiple scales method to resolve the equation of motion unstable regimes. They calculated the instability regions

in order to avoid of the exible cam mechanism of stable and dangerous working velocities. Cveticanin, [4]. described the mathematical model of cam-follower mechanism with two coupled non-linear, ordinary second-order differential equation. He developed new criteria for designing the cam profile based on the stable motion. Gue et al, [5]. applied the Fourier spectrum tool on cam acceleration based on frequency domain. The dynamic response at low frequency range has been related to different cam rotational speeds such as (700, 900, and 1100) rpm. Hsu and Pisano, [6]. Investigated the simulation of contact forces at three different speeds (660, 1650, and 2500) rpm of a finger-follower cam system. They determined the contact position between the cam and the follower by using the constrained equation method. The force at low speeds is employed to derive the dynamic Coulomb friction coefficients at contact points. chew and chuang, [7]. Implemented the generalized Lagrange multiplier method of cam-follower systems over a range of cam speeds. The results are checked by using a second approach of nonlinear programming technique. Fabien et-al, [8]. Explained a linear quadratic optimal control theory to design a high-speed of Dwell-Rise-Dwell (D-R-D) cams. Three approaches of D-R-D cam design are presented. In the first approach, the cam designed to be optimal at a fixed operating speed. In the second approach, the cam profile is determined by minimizing the sum of quadratic cost function over a range of discrete speeds. The third technique uses trajectory sensitivity minimization to design a cam which is insensitive to speed variations. Jiang et-al, [9]. Formulated the problems of minimizing vibrations in high-speed cam-follower systems over a range of speeds (800-3600) rpm. A universal Hermite cam displacement is suggested. Alzate et-al, [10] detected the sudden transition to chaos in a radial cam and a at faced follower. They observed that the follower detaches from the cam under the variation of cam rotational speeds. Yan et-al, [11]. Derived the equation of motion for a cam-follower system by using variable cam-input angular velocity. They found that peak values of follower output motion have been decreased by using proper cam-input trajectories. Bagci and Kurnool, [12]. Presented a Fourier series-Laplace transform to find the follower response at any time and at any cycle. They

Author: Assistant Professor Department of Mechanical Engineering San Diego State University 5500 Campanile Drive San Diego, CA 92182 1323 USA. e-mails: louaysabah1979@gmail.com, lalroomi@sdsu.edu

measured the critical cam speeds and follower jump conditions. Many researches have been done to reveal the effect of Lyapunov exponents on human-gait locomotion. The aim of this paper is to implement Lyapunov analyses to characterize stability of nonlinear dynamic.

II. SIMULATION PROCEDURE

The cam, roller-follower, and guides are designed in a Solid Works program using the experimental dimensions of existing mechanisms, [13]. A simulation was carried out for the planar case using the block commands. The general dimensions of the cam, follower, and its guides are measured in (mm) and are shown in Fig. 1. Different follower guide's clearances such as $C = 0.3, 0.5, 1, 1.5,$ and 2 mm have been used in the simulations. Fig. 2 shows the clearance between follower and its guide. The follower with clearance has three degrees of freedom translation in x, y directions and rotation about z axis. A marker has been stick on the follower by choosing a suitable point, which has the coordinates $(x: 0, y: 272$ mm, $z: 0)$, as indicated in Fig. 1. The force expression function is:

$$F = a - b \Delta \quad (1)$$

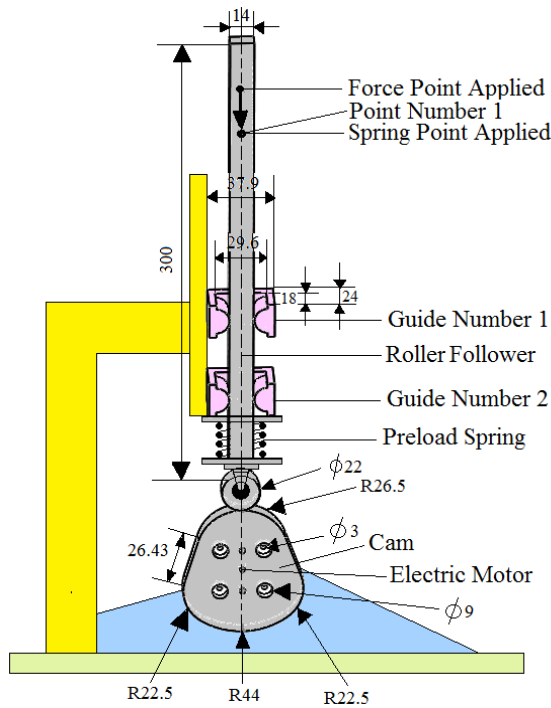


Figure 1: General Dimensions of Cam, Follower, and Guides

$$X(t) = [x(t), x(t + T), x(t + 2T), \dots, x(t + (d_E - 1)T)] \quad (3)$$

Time delay (T) and the embedding dimension (d_E) are necessary for the nonlinear analysis. A computer algorithms was carried out to calculate the time delay and the embedding dimension. Time delay is an integer number between two samples from time

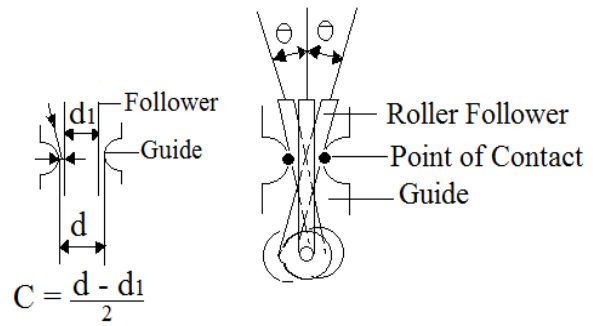


Figure 2: Schematic Diagram Illustrating Follower Guide's Clearance

Where, $a = 1.7508$ (N), $b = 0.038$ N/mm. The first term (a) represents the initial preload to avoid follower jumping during high speeds. The second term (b) represents the spring force varying with each position of the follower motion.

The contact force is defined as:

$$F_c = K \delta^n + \zeta \delta^n \dot{\delta} \quad (2)$$

The impact parameters that used in the Solidworks simulation are indicated in Table 1.

Table 1: Simulation Contact Parameters

Simulation Parameters		
Parameter's Definition	Value	Unit
Kinematic Sliding Velocity	10.16	mm/s
Kinematic Coefficient of Friction	0.2	—
Static Sliding Velocity	0.1	mm/s
Static Coefficient of Friction	0.3	—
Contact Bodies Stiffness	1100049.92	N/mm
Exponent	2	—
Max Damping	0.58839681	N/(mm/s)
Penetration	0.1	mm
Frame Per Second	500	—

III. QUANTIFYING LOCAL DYNAMIC STABILITY

The local dynamic stability of a cam-follower is quantified by calculating Lyapunov exponent values. Maximum finite-time Lyapunov Exponents were calculated based on the algorithm published by Rosenstein et al. [14]. The dynamic analysis was constructed by using the data of follower displacement. A valid state space is any vector space containing a sufficient number of independent coordinates, [15]. An appropriate state space can be reconstructed from a single time series as in the equation below:

series. If the time series represent a continuous on with samples taken every Δt seconds, then the delay parameter may be expressed as, [16]:

$$\tau = T \Delta t \quad (4)$$

Time delay was calculated from Average Mutual Information (AMI) algorithm. The time delay has been

chosen from first minimum of the (AMI) analysis, as shown in Fig. 3.

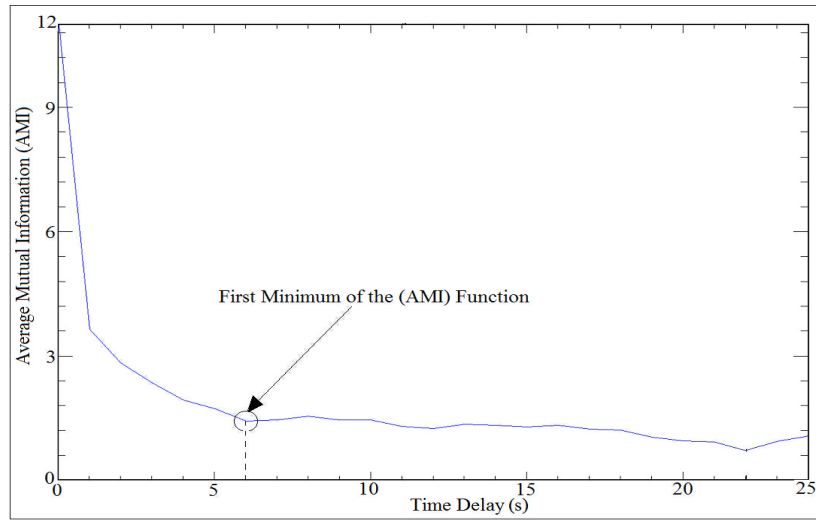


Figure 3: Average Mutual Information (AMI) Algorithm with Time Delay

With non-periodic systems and large value of τ , successive delay coordinates may become causally unrelated, and the reconstruction is no longer representative of the true dynamics, [16]. A related difficulty with attractor reconstruction involves the choice of d_E . The embedding dimension is the algorithm which determines the global number of a space data vectors. It converts a single time series into a multidimensional object in an embedding space vectors. d_E is usually estimated greater than twice the topological dimension (m) as:

$$d_E > 2m \quad (5)$$

Embedding dimension was computed from a Global False Nearest Neighbors (GFNN) algorithm. GFNN compares the distances between neighboring trajectories in the reconstructed state space at successively higher dimensions, as illustrated in Fig.4.

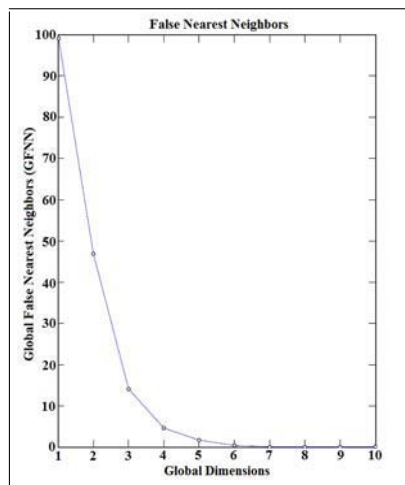


Figure 4: Global False Nearest Neighbors (GFNN) with Global Dimensions

The global dimension is chosen where the total percentage of false neighbors approaches zero, thus providing a sufficient number of coordinates to define the system state at all points in time, [17]. It can be suggested that it may be more appropriate to τ_w the reconstruction window, τ_w , rather than τ alone, in which τ_w and τ are interchanged as dictated by the particular context, as illustrated below: [18, 19, 20, 21]:

$$\tau_w = \tau(d_E - 1) \quad (6)$$

IV. EXPERIMENTAL SETUP

Our rig is based on a radial cam with an oscillating roller-follower. A spring with the elastic constant is used to maintain the contact between the cam and the follower. Figure 5 shows the curve fitting of spring stiffness values.

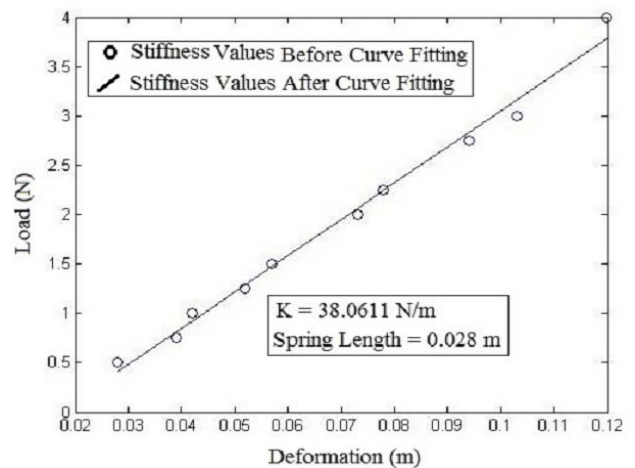


Figure 5: Load-Deflection Curve Fitting

The stiffness of the contact-retaining spring is determined to cause a minimum force pushing the follower system towards the cam. The system with follower's guide clearance $C = 0.3 \text{ mm}$ was used. The cam-follower mechanism has been manufactured by a 3D printing filament technique device. The mechanical device was shown to be appropriately coupled to electronic systems for the acquisition, storage and processing of experimental data, [10]. The main feature of the experimental set-up can be summarized as follows: (1) The cam motion was controlled by a brush-

less motor driven through an embedded controller. The angular position of the cam and the driving motor were assumed to be identical. (2) The measures of the cam and the follower positions are obtained through high-resolution optical encoders (markers). The marker has been stick on the follower which has the coordinates (x: 0, y: 272 mm, z: 0). (3) The OPTOTRAK / 3020 used to capture the motion through an infrared 3-D camera. The signals are analyzed using MATLAB program. The experimental rig was depicted in Fig. 6.

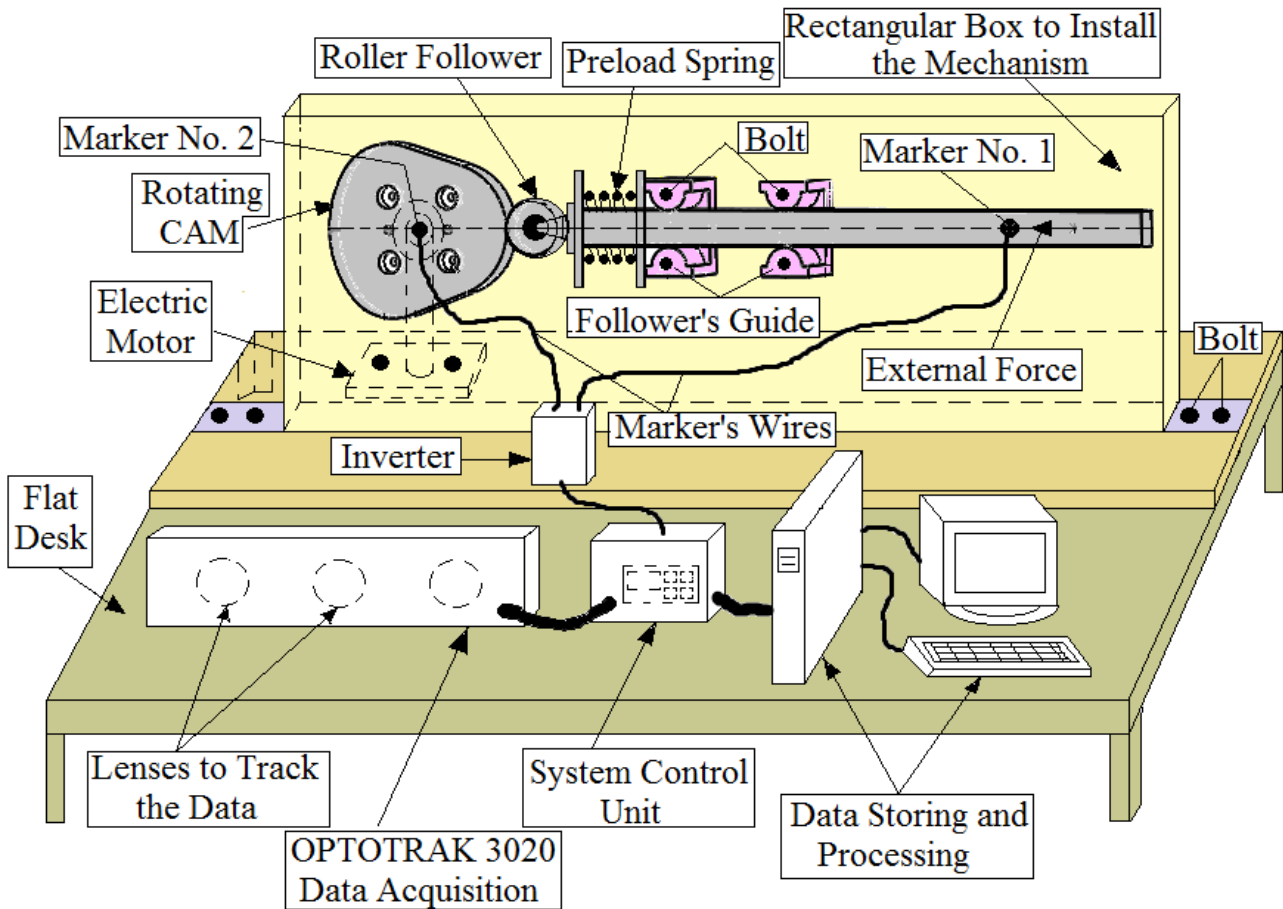


Figure 6: Experimental Rig Test

V. FINITE-TIME LYAPUNOV EXPONENT

Lyapunov exponents quantify the average exponential rate of divergence of neighboring trajectories in state space domain, and thus provide a direct measure of the sensitivity of the system to infinitesimal perturbations [15]. The maximum Lyapunov exponent (λ) can be defined by using the equation below:

$$d(t) = De^{\lambda t} \quad (7)$$

The Lyapunov exponent values were estimated from the slopes of linear fits to curves defined by:

$$y(i) = \frac{1}{\Delta t} \langle \ln[d_j(i)] \rangle \quad (8)$$

The Rosenstein method [14] estimates the largest Lyapunov exponents of a reconstructed attractor. The input to the program is a scalar follower displacement along with several parameters such as time delay and embedding dimension. The basic principle of this algorithm is to calculate the diverging ratio between trajectories in the state space domain, [22, 23]. The largest Lyapunov exponent was estimated from best-fit linear slopes of these local divergence

curves. The average local Lyapunov exponents determine the stability of the dynamic system using attractor trajectories. When the attractor is non-periodic, the trajectories diverge, on average, at an exponential rate characterized by the largest Lyapunov exponent [24]. The presence of a positive exponent is sufficient for diagnosing chaos and represents local instability in a particular direction. Larger values of Lyapunov exponents imply more divergence and variability of a system while smaller values reflect less divergence and variability. On the other hand, the lower positive Lyapunov exponents imply less sensitivity to perturbations. [25].

VI. RESULTS AND DISCUSSION

The verification of the follower linear displacement based on experiment and simulation techniques has been shown in Fig. 7. The simulation results were carried out using the y-direction because the simulation was obvious and clear. The verification was done by using $N = 400$ rpm of cam rotational speed. The system with follower's guide clearance $C = 0.3$ mm was used in the verification. In high-speed machinery, the jump is a situation where the cam and follower substantially scattered.

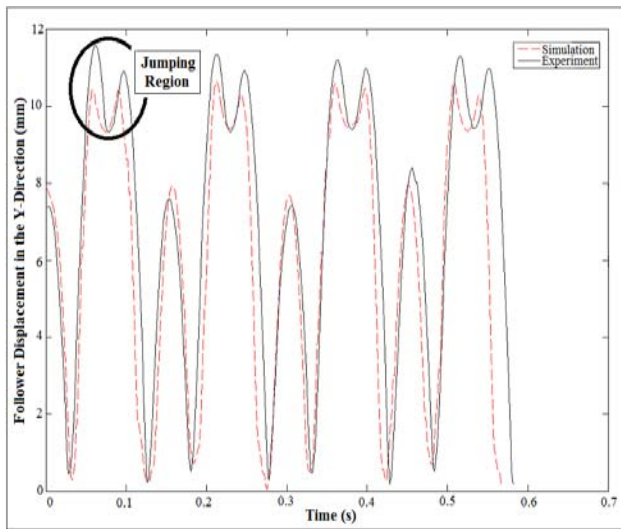


Figure 7: Follower Displacement in the Y-Direction

Table 2: Lyapunov Exponent Values Varying with Cam Rotational Speeds and Clearances

Cam Speed (rpm)	Clearance (0.5mm)	Clearance (1 mm)	Clearance (1.5 mm)	Clearance (2 mm)
200	0.284	0.211	0.217	0.181
300	0.192	0.28	0.208	0.416
400	0.384	0.321	0.124	0.128
500	0.239	0.191	0.267	0.277
600	0.348	0.369	0.203	0.179
700	0.241	0.266	0.307	0.283
800	0.236	0.3	0.366	0.349

Table (2) shows the simulation of Lyapunov exponent values varying with cam rotational speeds and follower guides' clearances. It can be observed that the largest Lyapunov exponent values are extremely constant for cam rotational speed $N = 200$ rpm and $N = 500$ rpm. The system with lowest Lyapunov exponent gives indication of local dynamic stability. The system with largest Lyapunov exponent represents the dynamic instability. The system with follower guide's clearance $C = 2$ mm and cam rotational speed $N = 300$ rpm has largest Lyapunov exponent. The system with follower guide's clearance $C = 1.5$ mm and cam speeds $N = 400$ rpm represents the local dynamic stability.

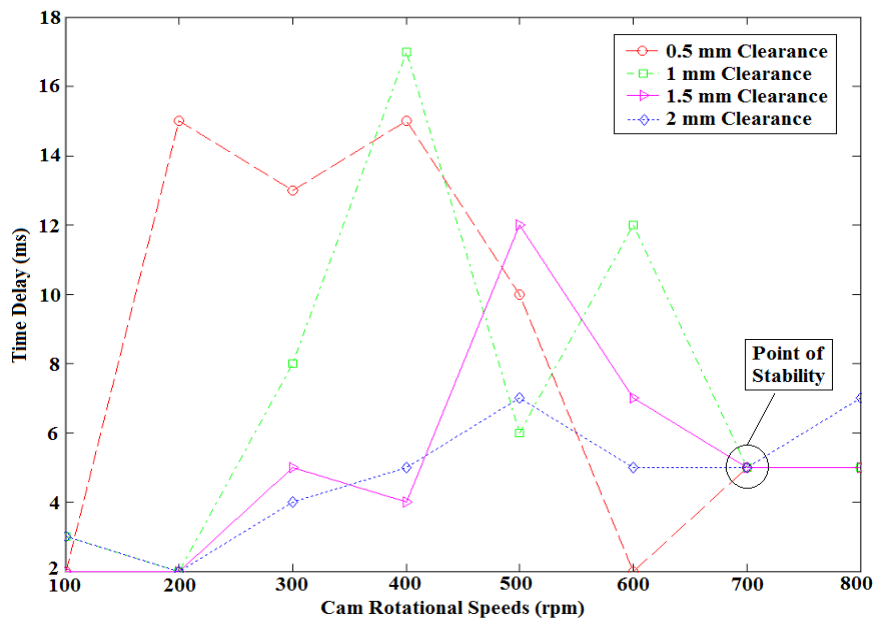
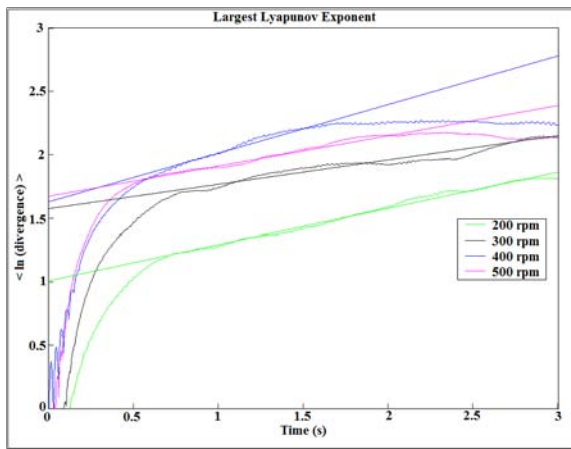


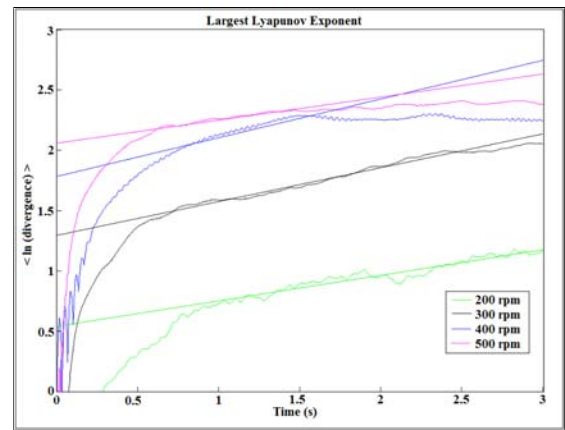
Figure 8: Illustrates the time delay variation with cam rotational speeds

The (AMI) algorithm has been done to find the time delay of cam-follower mechanism. At cam rotational speed $N = 700$ rpm the time delay is constant for whole values of cam rotational speeds. Figures 9a, 9b, 9c, and 9d have been done by using the Rosenstein method. The average logarithmic divergence for curve fitting has been touched the curve of average logarithmic divergence without any oscillation specially in Fig. 9a. The logarithmic divergence curve has been

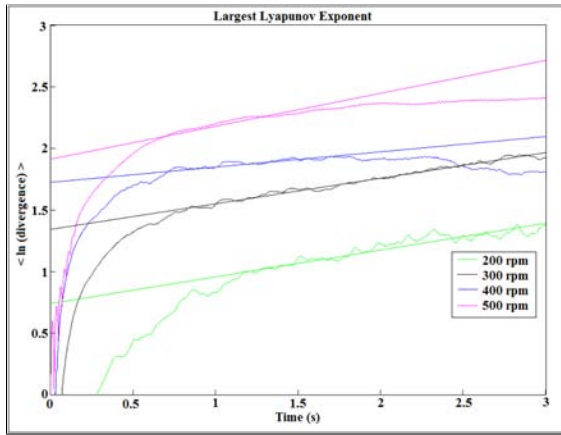
different cam rotational speeds and different follower guides clearances were investigated. The curve represents the average logarithmic divergence for follower attractor trajectories. The straight line represents the line of curvetting of least-square method which is given large Lyapunov exponent. The straight line of oscillation as in Fig. 9c, and 9d in which represents local dynamic instability. Figure 9a indicates to local dynamic stability.



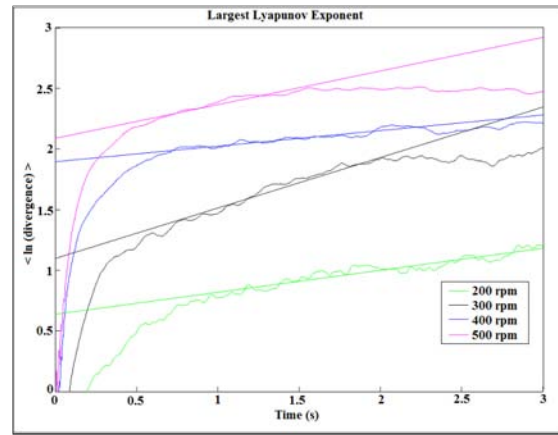
a) Average Logarithmic Divergence for Clearance $C = 0.5$ mm.



b) Average Logarithmic Divergence for Clearance $C = 1$ mm.



c) Average Logarithmic Divergence for Clearance $C = 1.5$ mm.

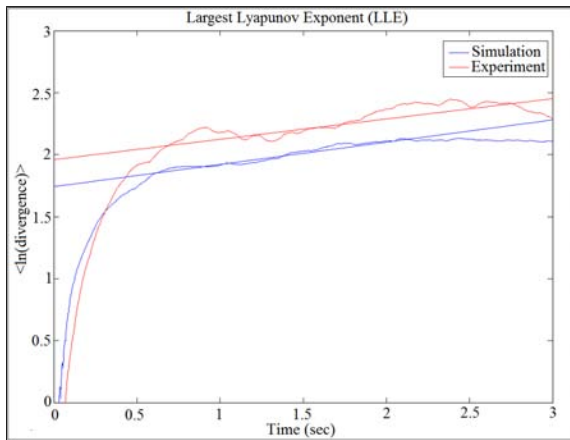


d) Average Logarithmic Divergence for Clearance $C = 2$ mm.

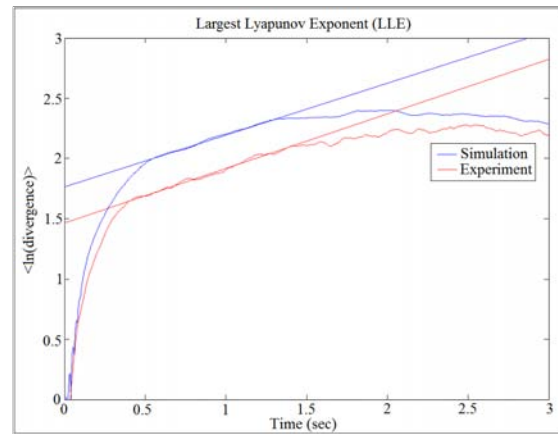
Figure 9: Average Logarithmic Divergence for Different Follower Guides' Clearances

Figures 10a, 10b, 10c, and 10d show the logarithmic divergence verification of largest Lyapunov exponent. Clearance $C = 0.3$ mm was considered in the verification. It can be seen from these figures that the average logarithmic divergence curve has been of

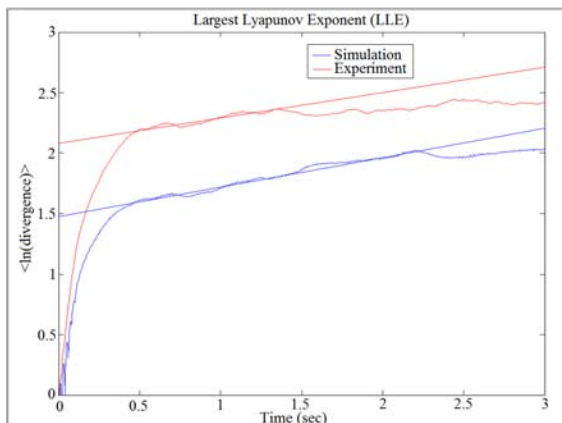
oscillation around the straight line of curve fitting Experimentally except in Figures 10b, and 10c. In the simulation analysis, the average logarithmic divergence curve is nearly tangent to the straight line of curve fitting.



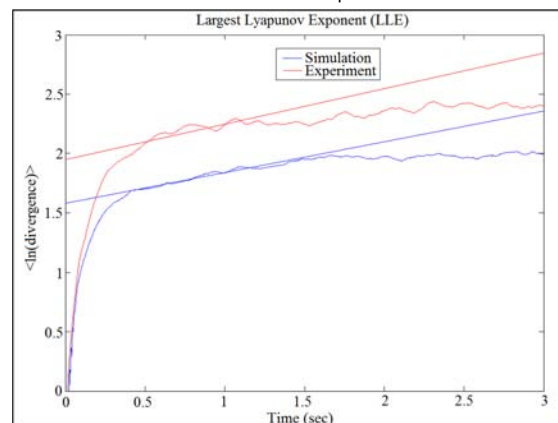
(a) Average Logarithmic Divergence Verification of $N = 340$ rpm.



(b) Average Logarithmic Divergence Verification of $N = 385$ rpm.



(c) Average Logarithmic Divergence Verification of $N = 410$ rpm.



(d) Average Logarithmic Divergence Verification of $N = 423$ rpm.

Figure 10: Average Logarithmic Divergence for Verification of Different Cam Rotational Speed.

Table (3) shows the large Lyapunov exponent values verification varying with cam rotational speeds. The system with followers guide clearance $C = 0.3 \text{ mm}$ was used in the verification. The system with cam speed

cam speed $N = 340 \text{ rpm}$ and Lyapunov exponent equal to (0.18) represents local dynamic stability. The system with cam speed $N = 385 \text{ rpm}$ and Lyapunov exponent equal to (0.431) indicates local dynamic instability.

Table 3: Lyapunov Exponent Values Verification for Different Cam Rotational Speeds

Cam Speed (rpm)	Simulation	Experiment	Error %
340	0.18	0.164	8.88
385	0.431	0.454	5.06
410	0.244	0.210	13.93
423	0.26	0.299	13.04

Figure 11 illustrates the Largest Lyapunov Exponent verses with cam rotational speed for different follower guides clearances. The system with follower guides clearance $C = 2 \text{ mm}$ and $N = 300 \text{ rpm}$ has

Lyapunov exponent equal to 0.42. The system with clearance $C = 1.5 \text{ mm}$ has Lyapunov exponent close to zero specially at $N = 100 \text{ rpm}$.

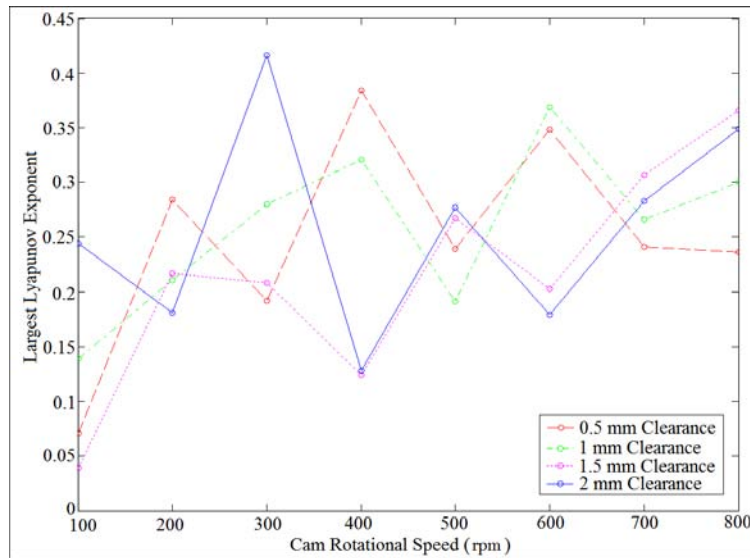


Figure 11: Largest Lyapunov Exponent Varying with Cam Rotational Speed and Different Follower Guides' Clearances

VII. CONCLUSIONS

This study analyze and discuss the largest Lyapunov exponent for the cam follower mechanism. Experimental part has been analyzed with data acquisition techniques using 3-D infrared system in order to measure the follower displacement. The numerical part has been done using Solidwork simulation. The system with lowest Lyapunov exponent gives indication of local dynamic stability. The system with largest Lyapunov exponent represents the dynamic instability.

The system with follower guide's clearance $C = 2 \text{ mm}$ and cam rotational speed $N = 300 \text{ rpm}$ has largest Lyapunov exponent. The system with follower guide's clearance $C = 1.5 \text{ mm}$ and cam speeds $N = 400 \text{ rpm}$ represents the local dynamic stability. The average logarithmic divergence curve has been oscillated around the straight line of curve fitting experimentally. In the simulation analysis, the average

logarithmic divergence curve is nearly tangent to the straight line of curve fitting.

Numenculture

- C: Follower guide's clearance.
- D: Average displacement between trajectories at $t=0$.
- F: External follower force.
- Fc: Contact force between cam and follower.
- K: Contact bodies stiffness.
- N: Cam rotational speed.
- n: Exponent.
- τ : Lag or reconstruction time delay.
- $X(t)$: Original one-dimensional data.
- $y(i)$: Curve fitting least square follower displacement data.
- dE: Embedding dimension.
- $d(t)$: Rate of change in the distance between nearest neighbors.
- $d_i(i)$: Euclidean distance between the pair of nearest neighbors.
- Δ : Follower linear displacement varying with time.
- Δt : Discrete time steps.

δ : Penetration.
 ζ : Damping ratio.
 τ : Delay parameter.
 τ_w : Length of the interval spanned by the first and last delay coordinates.
 λ : Lyapunov exponent.

RÉFÉRENCES

1. Y. Unlusoy, S. Tumer, Non-linear dynamic model and its solution for a high speed cam mechanism with coulomb friction, *Journal of sound and vibration* 169 (3) (1994) 395-407.
2. H. Hamidzadeh, M. Dehghani, Dynamic stability of flexible cam follower systems, *Proceedings of the Institution of Mechanical Engineers, Part K: Journal of Multi-body Dynamics* 213 (1) (1999) 45-52.
3. M. Tounsi, R. Hbaieb, F. Chaari, T. Fakhfakh, M. Haddar, Dynamic stability analysis of a flexible cam mechanism using a one-degree-of-freedom model, *Proceedings of the Institution of Mechanical Engineers, Part C: Journal of Mechanical Engineering Science* 223 (5) (2009) 1057-1068.
4. L. Cveticanin, Stability of motion of the cam follower system, *Mechanism and machine theory* 42 (9) (2007) 1238-1250.
5. J. Guo, W. Zhang, X. Zhang, Y. Cao, Dynamic and exciting analysis with modal characteristics for valve train using a flexible model, *Mechanism and Machine Theory* 78 (2014) 158-176.
6. W. Hsu, A. Pisano, Modeling of a finger-follower cam system with verification in contact forces, *Journal of Mechanical Design* 118 (1) (1996) 132-137.
7. C. Chuang, Minimizing residual vibrations in high-speed cam-follower systems over a range of speeds, *Journal of Mechanical Design* 117 (1995) 167-172.
8. B. Fabien, R. Longman, F. Freudenstein, The design of high-speed dwell-rise-dwell cams using linear quadratic optimal control theory, *Journal of Mechanical Design* 116 (3) (1994) 867-874.
9. J. Jiang, Y. Iwai, H. Su, Minimizing and restricting vibrations in high-speed cam-follower systems over a range of speeds, *Journal of Applied Mechanics* 74 (6) (2007) 1157-1164.
10. R. Alzate, M. Di Bernardo, U. Montanaro, S. Santini, Experimental and numerical verification of bifurcations and chaos in cam-follower impacting systems, *Nonlinear Dynamics* 50 (3) (2007) 409-429.
11. H.-S. Yan, M.-C. Tsai, M.-H. Hsu, A variable-speed method for improving motion characteristics of cam-follower systems, *Journal of Mechanical Design* 118 (2) (1996) 250-258.
12. C. Bagci, S. Kurnool, Exact response analysis and dynamic design of cam-follower systems using laplace transforms, *Journal of Mechanical Design* 119 (3) (1997) 359-369.
13. D. Planchard, *Solidworks 2017 Reference Guide*, SDC Publications, (2017).
14. M. T. Rosenstein, J. J. Collins, C. J. De Luca, A practical method for calculating largest lyapunov exponents from small data sets, *Physica D:Nonlinear Phenomena* 65 (1) (1993) 117-134.
15. J. B. Dingwell, J. P. Cusumano, Nonlinear time series analysis of normal and pathological human walking, *Chaos: An Interdisciplinary Journal of Nonlinear Science* 10 (4) (2000) 848-863.
16. M. T. Rosenstein, J. J. Collins, C. J. De Luca, Reconstruction expansion as a geometry-based framework for choosing proper delay times, *Physica D: Nonlinear Phenomena* 73 (1) (1994) 82-98.
17. J. Dingwell, J. Cusumano, P. Cavanagh, D. Sternad, Local dynamic stability versus kinematic variability of continuous overground and treadmill walking, *Journal of biomechanical engineering* 123 (1) (2001) 27-32.
18. D. S. Broomhead, G. P. King, Extracting qualitative dynamics from experimental data, *Physica D: Nonlinear Phenomena* 20 (2-3) (1986) 217-236.
19. Mees, P. Rapp, L. Jennings, Singular-value decomposition and embedding dimension, *Physical Review A* 36 (1) (1987) 340.
20. M. Albano, J. Muench, C. Schwartz, A. Mees, P. Rapp, Singular-value decomposition and the grassberger-procaccia algorithm, *Physical Review A* 38 (6) (1988) 3017.
21. J. Martinerie, A. M. Albano, A. Mees, P. Rapp, Mutual information, strange attractors, and the optimal estimation of dimension, *Physical Review A* 45 (10) (1992) 7058.
22. T. Schreiber, A. Schmitz, Surrogate time series, *Physica D: Nonlinear Phenomena* 142 (3) (2000) 346-382.
23. R. Hegger and H. Kantz, Practical implementation of nonlinear time series methods: The TISEAN package, *Chaos: An Interdisciplinary Journal of Nonlinear Science* 9 (2), (1999), 413-435.
24. J. Eckmann, D. Ruelle, Ergodic theory of chaos and strange attractors, *World Scientific Series on Nonlinear Science Series A* 16 (1995) 365-404.
25. K. Son, J. Park, S. Park, Variability analysis of lower extremity joint kinematics during walking in healthy young adults, *Medical engineering & physics* 31 (7) (2009) 784-792.